MAGMA (1994) 2, 51–59

Turbo spin-echo sequences in magnetic resonance imaging of the brain: Physics and applications

C. Fellner,[1]* F. Fellner,[2] R. Schmitt,[3] T. Helmberger,[3] N. Obletter,[4] and H. Böhm-Jurkovic[2]

[1]*Department of Radiology, University of Regensburg, Germany*
[2]*Department of Neuroradiology, Oberösterreichische Landesnervenklinik, Linz, Austria*
Departments of [3]*Radiodiagnostics and* [4]*MRI, Klinikum Ingolstadt, Germany*

Fast SE imaging provides considerable measure time reduction, high signal-to-noise ratios as well as similar contrast behavior compared to conventional SE sequences. Besides TR and TE_{eff}, echo train length (ETL), interecho time τ, and *k*-space trajectory determine image contrast and image quality in fast SE sequences. "True" proton density contrast (CSF hypointense) and not too strong T2 contrast are essential requirements in routine brain MRI. A Turbo SE sequence with very short echo train length (ETL = 3), short TE_{eff} and short interecho time (17 ms), and TR = 2000 ms was selected for proton density contrast; a Turbo SE sequence with ETL = 7, TE_{eff} = 90 ms, τ = 22 ms, and TR = 3250 ms was selected for T_2-weighted images. Using both single-echo Turbo SE sequences yielded 50% measure time reduction compared to the conventional SE technique. Conventional SE and optimized Turbo SE sequences were compared in 150 patients resulting in very similar signal and contrast behavior. Furthermore, reduced flow artifacts in proton density—and especially in T_2-weighted Turbo SE images—and better contrast of high-intensity lesions in proton density-weighted Turbo SE images were found. Slightly reduced edge sharpness—mainly in T_2-weighted Turbo SE images—did not reduce diagnostic reliability. Differences between conventional and Turbo SE images concerning image contrast and quality are explained regarding special features of fast SE technique.

Keywords: MRI, brain, FSE, fast spin-echo sequences, TSE, turbo spin-echo sequences, signal behavior

INTRODUCTION

Depending on the repetition time TR and the echo time TE, spin-echo (SE) sequences provide T_1-, T_2- or proton density (PD)-weighted images. Long acquisition times—especially for T_2-weighted SE images—are an important drawback of this standard sequence. Several fast imaging techniques have been proposed including gradient-echo (GE), fast spin-echo (FSE) and echo planar imaging (EPI). Using short repetition and echo times yields an essential reduction of measure time in GE sequences [1–3]. In ultrafast GE imaging (TurboFLASH) [4]—using very short TR and TE and a very low flip angle—the spin system has to be prepared once before the excitation to produce T_1-, T_2- or PD-contrast. In SE as well as in GE imaging, only one phase encoding step is performed during a TR period, whereas in FSE [5–7] or rapid acquisition with relaxation enhancement (RARE) [8, 9] and EPI [10] techniques several or even all lines of the *k*-space are measured between two excitation pulses. The *k*-space trajectory not only influences the image contrast but also image quality: reduced or even increased edge sharpness in FSE imaging depends on the manner of *k*-space filling. Signal and contrast behavior is mainly determined by low-phase encoding steps encoding the center of the *k*-space; therefore, TE_{eff} denotes the echo time for the central phase encoding step (Fig. 1). Furthermore, echo train length (ETL) and interecho time τ (echo spacing) are important parameters for image contrast and quality in FSE imaging.

Up to now, most studies concerning fast SE or Turbo

* *Address for correspondence: Institut für Röntgendiagnostik, Klinikum der Universität Regensburg, Franz-Josef-Strauß-Allee 11, 93042 Regensburg, Germany.* *Additional reprints of this chapter may be obtained from the Reprints Department, Chapman & Hall, One Penn Plaza, New York, NY 10119.*
Received 24 September 1993.

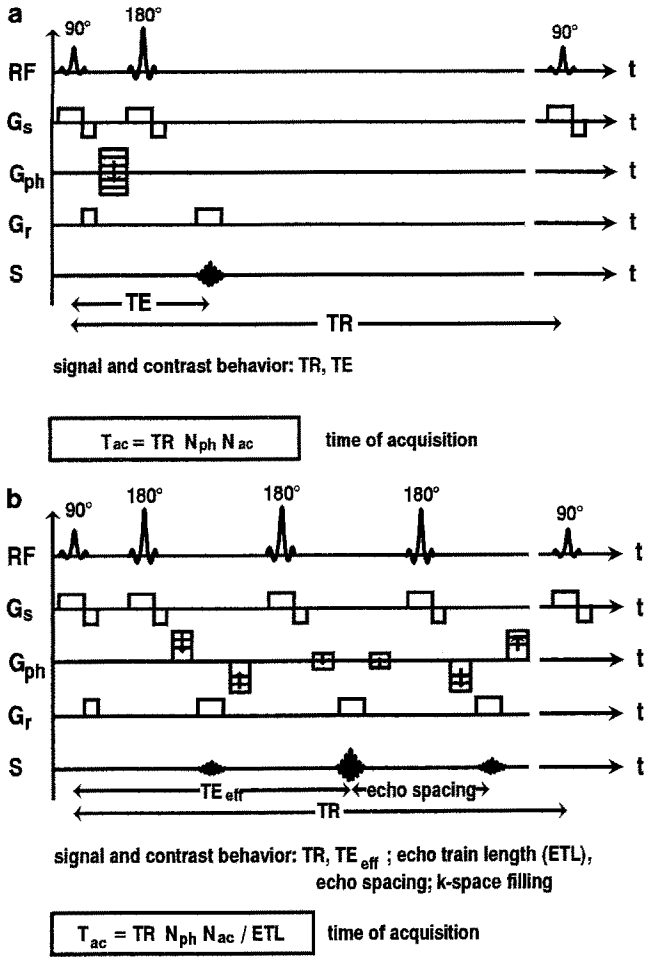

Fig. 1. Sequence diagram, measurement parameters determining signal behavior, and time of acquisition. (a) SE sequence; (b) TSE sequence.

SE (TSE) imaging of the brain were performed at 1.5 T comparing (mildly or strongly) T_2-weighted images [11–15]. The aim of this study was to obtain equivalent PD- and T_2-contrast of TSE sequences for routine brain magnetic resonance imaging (MRI) at 1.0 T compared to conventional SE imaging. The optimization included a measure time reduction of about 50%, maintaining good image quality and "true" PD-contrast, which is important for delineation of periventricular and subcortical lesions. Signal and contrast behavior, flow artifacts, and delineation of small structures were compared for optimized TSE and conventional SE technique.

METHODS

All examinations were performed on a 1.0-T scanner (Siemens Magnetom "Impact") using a quadrature transmit/receive head coil. In a pilot study, several single-echo and dual-echo TSE pulse sequences were evaluated in healthy volunteers to optimize PD- and T_2-contrast compared to our standard SE sequence (TR = 2200 ms, TE = 13–80 ms) for routine brain imaging.

We selected two single-echo TSE sequences: for PD-weighted images, a TSE sequence with ETL = 3, TR = 2000 ms, TE_{eff} = 17 ms, and τ = 17 ms; for T_2-contrast, a TSE sequence with ETL = 7, TR = 3250 ms, TE_{eff} = 90 ms, and τ = 22 ms. The time of acquisition for PD- and T_2-weighted TSE sequences was 2 min 53 s and 2 min 5 s, respectively, whereas the SE technique required 9 min 26 s imaging time. In each case the measurement included 19 axial slices with a slice thickness of 6 mm, a 1.2-mm slice gap, and a matrix size of 256^2 with one acquisition.

The optimized TSE sequences as well as the standard SE sequence were compared in routine brain examinations of 150 patients. Of these patients, 109 patients revealed pathologic changes: arteriosclerotic white matter lesions (n = 35), neoplastic changes (n = 25), inflammatory diseases (n = 22), infarctions (n = 10), hematomas (n = 9), neurodegenerative diseases (n = 3), and closed lip schizencephalopathies (n = 24); in 41 patients, no lesions were found.

In all patients, signal intensities of gray and white matter and CSF were measured in operator-defined regions of interest (ROIs) and signal-to-noise ratios (S/Ns) were calculated. The measurement of background noise was performed in large circular regions free of artifacts outside the patient; the standard deviation in this area was used as the noise value (N). The ROIs for noise and all anatomical structures were positioned within the same slice. The contrast-to-noise ratio (C/N) for gray and white matter was calculated:

$$C/N = (S_{GM} - S_{WM})/N \quad (1)$$

where S_{GM} and S_{WM} are the signal intenities of gray and white matter, respectively.

Furthermore, gray/white matter contrast, flow artifacts, and delineation of small structures were analyzed by three independent radiologists (F.F., R.S., T.H.) using a scale ranging from 1 to 5. A 1 denoted very low contrast and a 5 very high contrast between gray and white matter. Flow artifacts were evaluated ranging between "no artifacts" (1) and "severe artifacts" (5). Delineation of vessels and contrast of high-intensity lesions (inflammatory and arteriosclerotic white matter lesions) were rated separately, again using a scale between 1 and 5.

Mean values and standard deviations were calculated for the results of ROI measurements as well as for the results of visual evaluation. A paired t-test (Student) was performed to determine the statistical

Table 1. Results of ROI evaluation: mean values (n = 150) and standard deviation of signal intensities, S/N, noise, and C/N (gray matter/white matter) in PD- and T_2-weighted SE and TSE images

	SE PD	TSE PD	SE T_2	TSE T_2
$S_{\text{gray matter}}$	1280.5 ± 58.6	1114.2 ± 47.2[a]	509.6 ± 34.6	630.2 ± 49.2[a]
$S_{\text{white matter}}$	1142.7 ± 56.0	985.6 ± 48.9[a]	392.3 ± 33.9	458.1 ± 46.1[a]
S_{CSF}	788.0 ± 36.8	725.4 ± 38.0[a]	660.6 ± 38.1	1096.5 ± 52.1[a]
Noise	13.3 ± 1.3	12.1 ± 1.4[a]	8.9 ± 0.9	11.8 ± 1.2[a]
$S/N_{\text{gray matter}}$	97.4 ± 10.3	93.4 ± 9.8[a]	58.1 ± 6.9	54.1 ± 6.1[a]
$S/N_{\text{white matter}}$	87.0 ± 9.6	82.7 ± 9.0[a]	44.6 ± 5.6	39.3 ± 5.2[a]
S/N_{CSF}	60.0 ± 6.6	61.1 ± 6.9[b]	75.1 ± 8.2	94.3 ± 9.8[a]
$C/N_{\text{gray/white matter}}$	10.5 ± 4.0	10.8 ± 4.1[c]	13.3 ± 4.9	14.8 ± 4.6[a]

Statistics (paired Student's t-test): [a]$p < 0.001$, [b]$p < 0.02$, [c]not significant.

significance between the results of SE and TSE sequences.

RESULTS

At the beginning of this study, dual-echo TSE sequences yielded only mildly or strongly T_2-weighted images. To realize "true" PD-contrast—showing CSF hypointense compared to white matter—a single-echo TSE sequence with a very short ETL (ETL = 3) had to be selected. An ETL of 7 for T_2-weighted TSE images was used to reduce the time of acquisition to about 50% for both TSE sequences compared to conventional SE imaging. For T_2-weighted TSE images, the repetition time TR had to be prolonged up to 3250 ms to obtain 19 slices. Owing to longer TR, T_2-contrast was enhanced in T_2-weighted TSE images compared to SE images.

Mean values of signal intensities for gray and white matter and CSF including standard deviation for both sequence types and statistical significance are presented in Table 1. For all tissues, signal intensities were significantly lower in PD-weighted TSE than in SE images: the signal reduction was more pronounced for gray (−13.0%) and white matter (−13.8%) than for CSF (−8.0%). In contrast to PD-weighted images, T_2-weighted TSE images showed higher signal intensities for gray (+23.7%) and white (+16.8%) matter; for CSF, the signal gain was even 66% (see also Fig. 4).

The mean values of noise were 13.3 and 8.9 in PD- and T_2-weighted SE images, respectively, and 12.1 and 11.8 in PD- and T_2-weighted TSE images, respectively.

Caused by different noise values for SE and TSE images, different S/N behavior resulted (Table 1): S/Ns in PD-weighted TSE images were slightly lower for gray and white matter and only a little bit higher for CSF compared to SE images. T_2-weighted TSE images yielded higher S/N for CSF, but lower S/N for gray and white matter.

Contrast between gray and white matter was equivalent in PD-weighted SE and TSE images. Contrary to equivalent contrast in T_2-weighted images for visual evaluation, the measurement of C/N in ROIs resulted in significantly higher contrast for TSE images. Table 2 summarizes the results of visual evaluation. Flow artifacts were judged to be clearly reduced in T_2-weighted TSE images; this advantage was found to be less pronounced in PD-weighted TSE images (Fig. 2). TSE images—in particular T_2-weighted TSE images—were inferior in depicting small vessels. Contrast between small arteriosclerotic white matter lesions and surrounding tissue was higher in PD-weighted and lower in T_2-weighted TSE images compared to corresponding SE images. Equivalent results were found for inflammatory white matter lesions (Fig. 3).

Table 2. Results of visual evaluation for PD- and T_2-weighted SE and TSE images

	SE PD	TSE PD	SE T_2	TSE T_2
Contrast gray/white matter	4.31 ± 0.73	4.25 ± 0.70[c]	4.13 ± 0.75	4.16 ± 0.72[c]
Contrast vessels/surrounding tissue	3.83 ± 0.43	3.59 ± 0.54[b]	4.03 ± 0.44	3.36 ± 0.50[a]
Contrast arteriosclerotic lesions/white matter	3.19 ± 0.58	3.94 ± 0.59[a]	4.74 ± 0.44	4.24 ± 0.47[a]
Flow artifacts	2.73 ± 0.97	2.46 ± 0.85[b]	2.22 ± 0.83	1.07 ± 0.26[a]

Mean values (n = 150) and standard deviation using a scale between 1 and 5 for contrast (1 = no contrast, 5 = high contrast) and flow artifacts (1 = no artifacts, 5 = severe artifacts). Statistics (paired Student's t-test): [a]$p < 0.001$, [b]$p < 0.02$, [c]not significant.

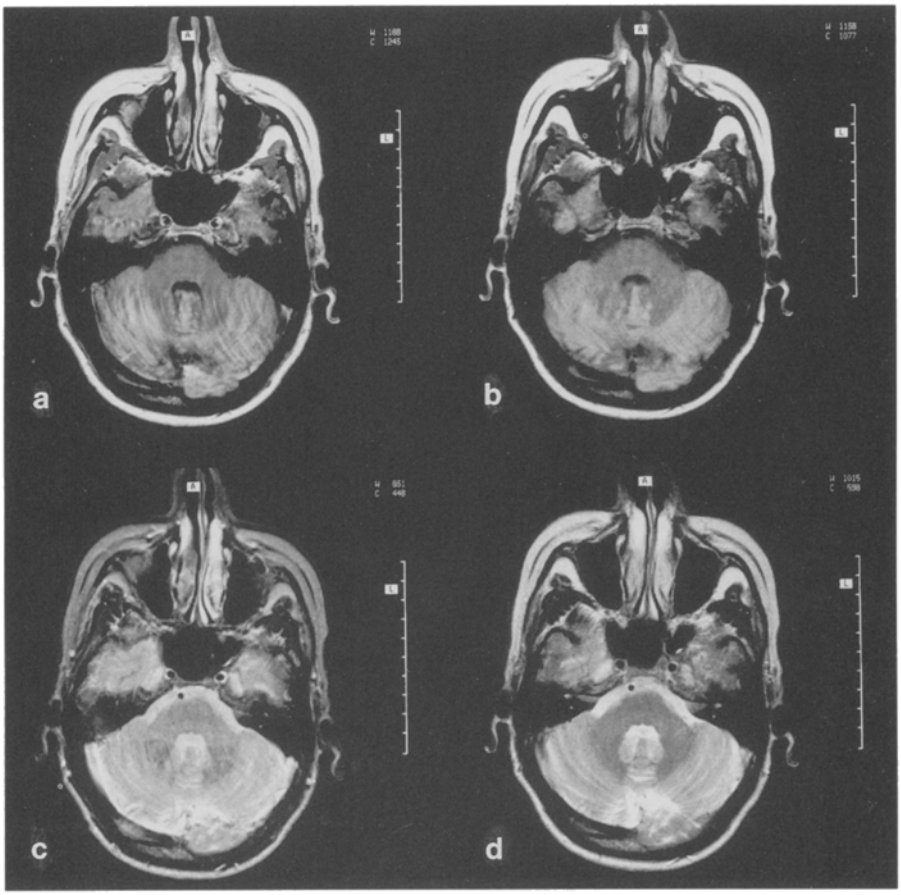

Fig. 2. Reduced flow artifacts in PD-weighted and especially in T_2-weighted TSE images compared to corresponding SE images. (a) PD-weighted SE image (TR = 2200 ms, TE = 13 ms; dual-echo). (b) PD-weighted TSE image (TR = 2000 ms, TE = 17 ms, ETL = 3; single-echo). (c) T_2 -weighted SE image (TR = 2200 ms, TE = 80 ms; dual-echo). (d) T_2-weighted TSE image (TR = 3250 ms, TE = 90 ms, ETL = 7; single-echo).

DISCUSSION

A dual-echo SE sequence with a repetition time of 2200 ms and echo times of 13 and 80 ms had proved to be optimal for routine brain MRI because periventricular and subcortical lesions can be delineated in PD-weighted as well as in T_2-weighted images. Furthermore, differentiation of CSF versus edema is possible in T_2-weighted SE images due to lower signal intensity for CSF compared to edema.

To realize "true" PD-contrast in TSE images, the signal intensity of CSF can be reduced, suppressing T_2 relaxation effects. We, therefore, shortened the repetition time (TR = 2000 ms) and chose TE_{eff}, ETL, and τ as short as possible. Applying these measurement parameters, the signal intensity of CSF was still higher in TSE than in SE images but was hypointense compared to white matter.

Differences in signal and contrast behavior between SE and TSE images can partially be understood by taking into account different repetition and echo times. Therefore, mean values of signal intensities measured in SE images were extrapolated to those measurement parameters used in TSE sequences with the well-known formula

$$S \sim \rho \exp\left(-\frac{TE}{T_2}\right)\left[1 - \exp\left(-\frac{TR}{T_1}\right)\right] \qquad (2)$$

The proton density ρ was kept constant and T_1 and T_2 relaxation times according [16–18] were applied: T_1 = 810 ms and T_2 = 101 ms for gray matter, T_1 = 680 ms and T_2 = 92 ms for white matter, and T_1 = 1390 ms and T_2 = 140 ms for CSF. Very different relaxation times have been published for CSF; the relaxation times used above might be too short, and, therefore, signal intensity for SE 3250/90 might be too low. Figure 4 represents the results of this extrapolation together with mean values of measured signal intensities for gray and white matter and for CSF in PD- and T_2-weighted SE and TSE images. Similar results were

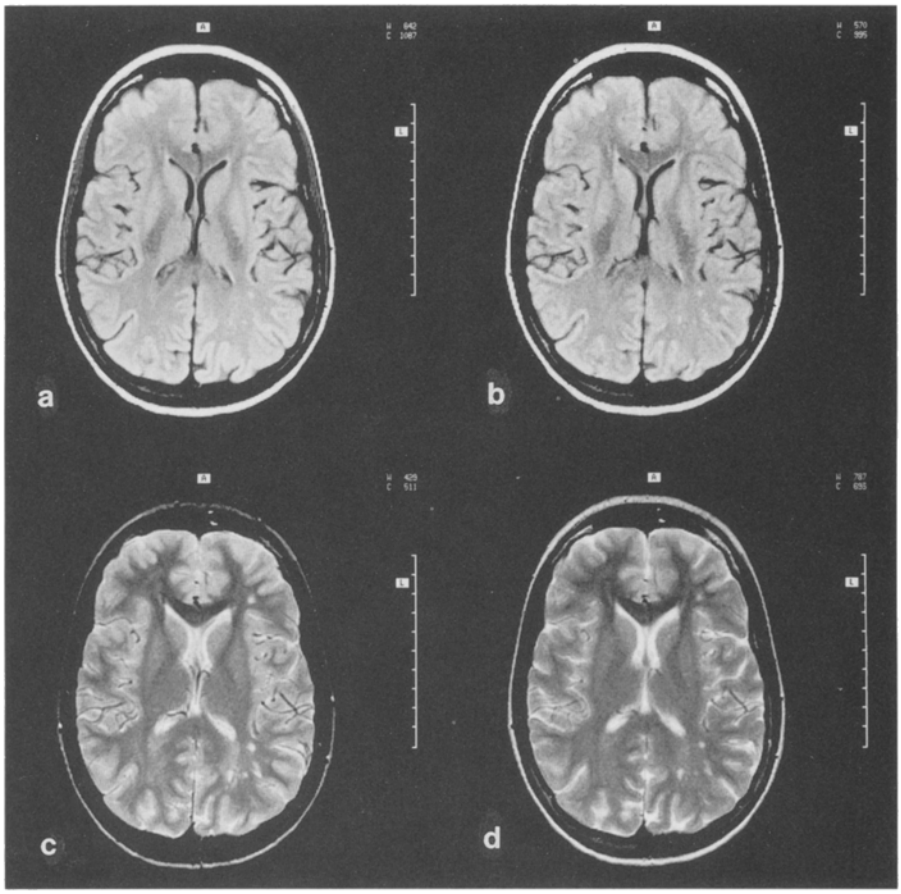

Fig. 3. Patient with multiple sclerosis: Inferior lesion contrast in T_2-weighted TSE images, but superior contrast in PD-weighted TSE images compared to corresponding SE images. Note slightly reduced edge sharpness of small lesions and vessels in T_2-weighted TSE images. (a) PD-weighted SE image (TR = 2200 ms, TE = 13 ms; dual-echo). (b) PD-weighted TSE image (TR = 2000 ms, TE = 17 ms, ETL = 3; single-echo). (c) T_2-weighted SE image (TR = 2200 ms, TE = 80 ms; dual-echo). (d) T_2-weighted TSE image (TR = 3250 ms, TE = 90 ms, ETL = 7; single-echo).

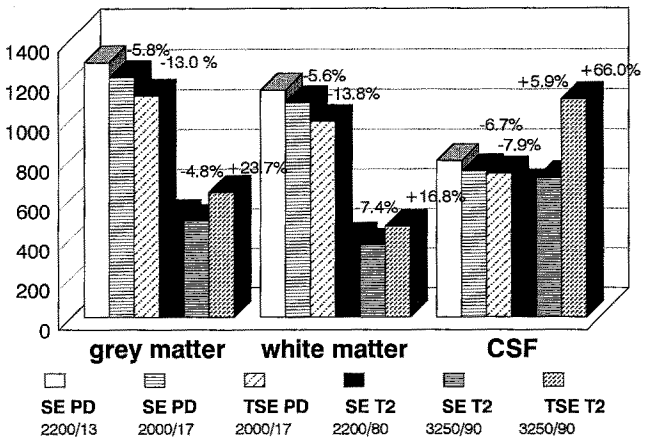

Fig. 4. Mean values of signal intensities for gray and white matter and CSF in PD- and T_2-weighted SE and TSE images including extrapolated values for SE 2000/17 and SE 3250/90.

found in healthy volunteers ($n = 6$) by comparing signal intensities in SE sequences with 2200/13.80 and 2000/17, respectively, 3250/90: signal reduction in PD-weighted images for gray and white matter and CSF (−0.6%, −1.2%, −4.6%); signal gain for CSF (+31.5%) in T_2 -weighted images, but signal reduction for gray and white matter (−1.0%, −4.8%). This extrapolation is only a rough estimation: signal and contrast behavior is mainly determined by the signal of central *k*-space lines, i.e., the effective echo time TE_{eff}, but the remaining echoes within an TSE echo train also contribute to the signal according to their position in the *k*-space. Thus, signal intensities in PD-weighted TSE images are reduced owing to longer TE and shorter TR compared to SE images and, furthermore, owing to the influence of two later echoes. Signal loss caused by a later echo time (90 ms instead of 80 ms) is compensated only for CSF prolonging TR from 2200 to 3250 ms. Despite this signal

reduction, signal gain due to earlier echoes is higher than signal loss due to later echoes within a symmetrical echo train used in T_2-weighted TSE sequences resulting in higher signals in T_2-weighted TSE than in SE images.

Additionally, two types of saturation effects are important in multislice imaging: direct saturation effects caused by imperfect excitation profiles and magnetization transfer (MT) effects [19, 20]. Using a "train" of off-resonant 180° radio frequency (RF) pulses, MT effects are more pronounced in TSE than in SE multislice imaging. Figure 5 illustrates saturation effects varying the number of slices in SE and TSE imaging: direct saturation effects should be equivalent in SE and TSE imaging; therefore, increased saturation effects in TSE images can be attributed to magnetization transfer. Reducing the number of slices yields a considerable increase of signal intensities for gray and white matter in both sequence techniques, whereas no significant changes were found for CSF (except for the single slice technique where no direct saturation is possible). Signal gain—and, therefore, MT effects—is more pronounced in the T_2-weighted TSE sequence (ETL = 7) than in the PD-weighted TSE sequence (ETL = 3). MT and direct saturation effects can be diminished, performing "interleaved" imaging, i.e., collecting first the odd slices and then the even slices [11]. We employed the interleaved mode in both sequence types to gain more signal. Reduction of signal intensities of gray and white matter in TSE compared to extrapolated SE values was more pronounced than for CSF: MT effects are only significant for gray and white matter but not for CSF.

Our results for signal intensities in SE and TSE images seem to be in contradiction with results published earlier: Ahn *et al.* [12] reported similar signal intensities for gray and white matter in PD-weighted TSE (2000/15) and in SE (2000/30) images and lower signal intensities in T_2-weighted TSE (2000/90) than in SE (2000/80) images. Once again, differences in TR and TE have to be taken into account; additionally, *k*-space filling might be different for both TSE sequence types.

A higher noise level was measured in PD-weighted SE images than in TSE images, although both sequences use identical bandwidths (130 Hz/pixel). Owing to reduced bandwidth (45 Hz/pixel) for the second echo of the SE sequence, T_2-weighted SE images showed less noise than corresponding TSE images (bandwidth 130 Hz/pixel). However, reduction of noise was lower than expected. Generally, noise was lower in TSE than in SE images, assuming identical bandwidth. These results differ from those published by Jones *et al.* [13, 14] who found a higher noise level

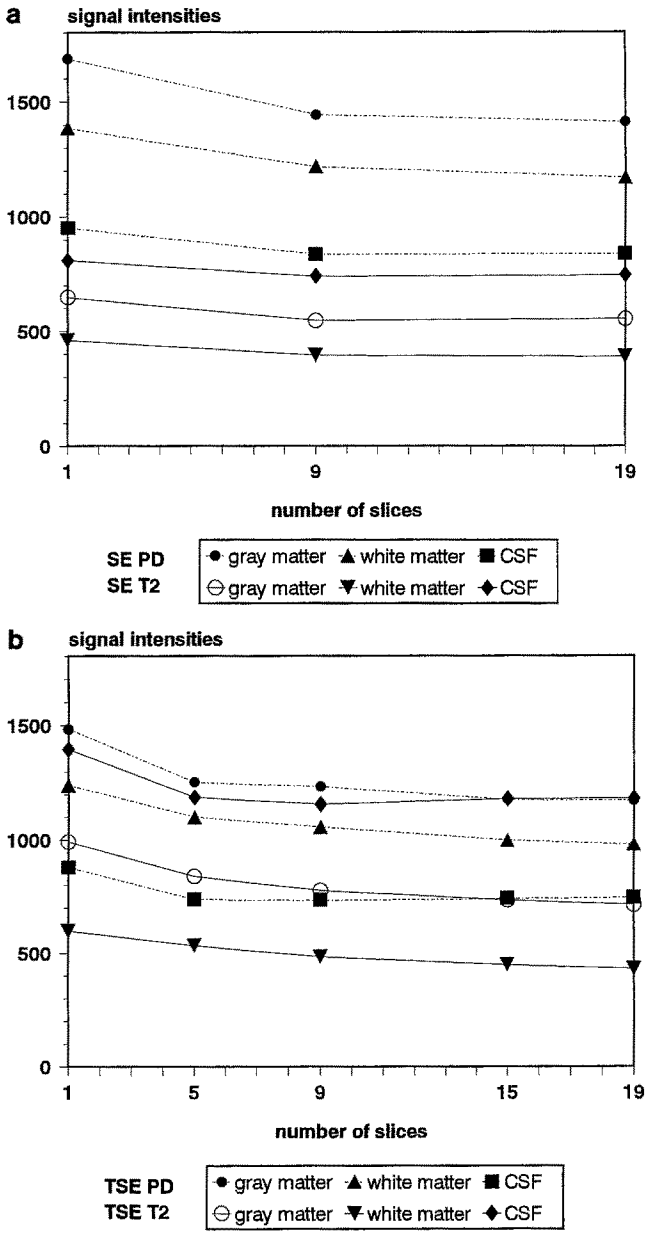

Fig. 5. Increase of signal intensities for gray and white matter and CSF decreasing the number of slices in PD- and T_2-weighted SE and TSE sequences. (a) PD- and T_2-weighted SE images (dual-echo sequence). (b) PD- and T_2-weighted TSE images (single-echo sequences).

in the phase encoding direction for TSE images. For our TSE images, there was no difference between noise in the phase encoding direction and noise in a circular region. Higher noise in PD-weighted SE and T_2-weighted TSE images results in a similar S/N for SE and TSE sequences—except for very high signal intensity and S/N of CSF in T_2-weighted TSE images. An advantage of T_2-weighted TSE images was reduced chemical shift artifacts due to higher bandwidth com-

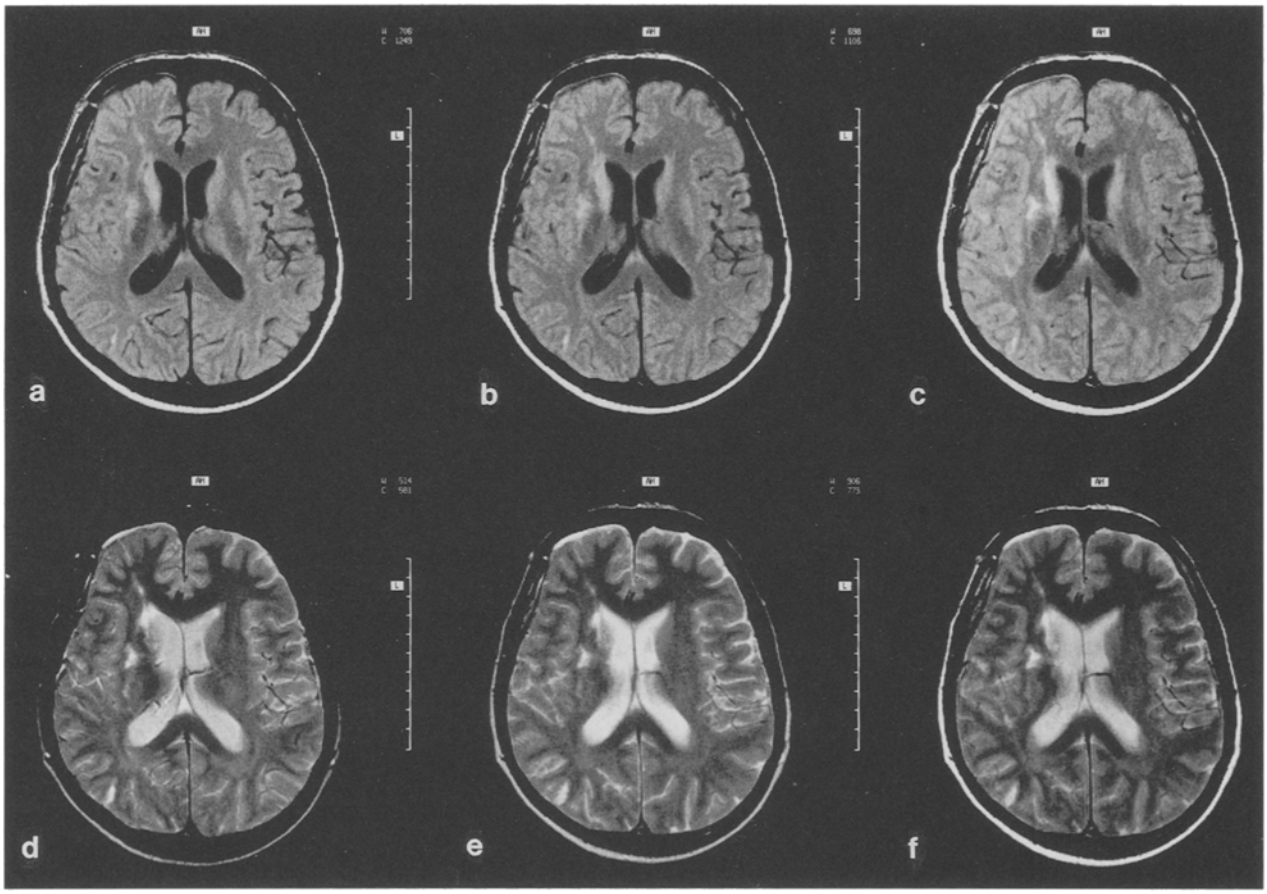

Fig. 6. Patient with periventricular and subcortical microischemic lesions. Higher contrast in PD-weighted single-echo images and especially in dual-echo TSE images compared to corresponding SE images. Better delineation of periventricular lesions in dual-echo than in single-echo T_2-weighted TSE images. (a) PD-weighted SE image (TR = 2200 ms, TE = 13 ms; dual-echo). (b) PD-weighted TSE image (TR = 2000 ms, TE = 17, ETL = 3; single-echo). (c) PD-weighted TSE image (TR = 2100 ms, TE = 14 ms, ETL = 5; dual-echo). (d) T_2-weighted SE image (TR = 2200 ms, TE = 80 ms; dual-echo). (e) T_2-weighted TSE image (TR = 3250 ms, TE = 90 ms, ETL = 7; single-echo). (f) T_2-weighted TSE image (TR = 2100 ms, TE = 85 ms, ETL = 5; dual-echo).

pared to corresponding SE images—maintaining sufficiently high S/N.

C/N values for gray and white matter were found to be superior in T_2-weighted TSE images and equivalent in PD-weighted SE and TSE images—in opposition to Ahn *et al.* [12]. The contradiction between the results of our visual evaluation of gray matter/white matter contrast and C/N values in T_2-weighted SE and TSE images can be understood taking into account the following: different windowing for TSE images compared to SE images is necessary to avoid too high signal intensities of CSF resulting in reduced gray/white matter contrast.

Considerably less flow artifacts were observed in T_2-weighted TSE than in SE images, although gradient moment nulling was used in both sequences. This effect might be attributed to the higher number of rephasing 180° RF pulses in TSE sequences. The advantage of reduced flow artifacts is less pronounced in PD-weighted TSE images.

Inferior contrast between vessels and surrounding tissues in TSE images can be attributed to the well-known effect of reduced edge sharpness in the phase encoding direction for TSE sequences [8, 21]. This kind of blurring is caused by different echo times for different phase encoding steps and is described by the point spread function (PSF). For conventional SE imaging, the PSF is a δ-function. Especially for long ETL, long τ, short TE_{eff} and for tissues with short T_2, the PSF broadens [21]. This effect of reduced edge sharpness was more pronounced for the longer echo train in T_2-weighted TSE images.

Similar behavior was observed for small lesions. However, PD-weighted TSE images yielded better contrast of high intensity lesions than conventional images (Figs. 3 and 6). Increased T_2 influence due to

later echoes and MT effects reducing the signal of white matter but not of lesions can explain this result.

A disadvantage of TSE sequences is reduced contrast of some iron-containing structures and calcifications [14, 15, 22]; therefore, we routinely use a gradient echo sequence (2D FLASH multislice, $\alpha = 90°$) in addition to the TSE sequences described earlier. Besides high image quality and similar signal and contrast behavior compared to conventional SE imaging, this TSE technique—consisting of two single-echo TSE sequences—is well suited for routine brain MRI [22]. True PD-contrast—an essential tool for depicting periventricular and subcortical lesions (Fig. 6)—is difficult to realize with dual-echo TSE sequences with good image quality and a sufficient number of slices [12]. For that reason we selected two single-echo TSE sequences. Meanwhile, an improved gradient system provides a gradient field strength up to 15 mT/m: TSE sequences with shorter echo and interecho times can be realized; thus, a dual-echo TSE sequence with ETL = 5 (TR = 2100 ms, TE_{eff} = 14, 85 ms, including 19 slices) yields a further decrease of measuring time (3 min 35 s) maintaining good PD- and T_2-contrast (Fig. 6) [23].

CONCLUSION

Optimized TSE sequences provide very similar signal and contrast behaviors compared to conventional dual-echo SE sequences, reducing the time of acquisition to 50%. True PD-contrast and increased T_2-contrast compared to SE images could be realized using two single-echo TSE sequences. "True" PD-contrast—showing CSF hypointensive compared to white matter—is an important requirement for routine brain MRI. Owing to improved hardware and software, a new dual-echo TSE sequence can also yield high-quality PD- and T_2-weighted images reducing the measuring time to 3 min 35 s for 19 slices.

Differences in signal and contrast behaviors between conventional and TSE imaging can be understood taking into account different imaging parameters and special properties of fast spin-echo imaging: *k*-space ordering and central echoes, but although influence of those echoes filling the *k*-space, interecho time and magnetization transfer effects are the most important features.

Reduction of flow artifacts—especially in the posterior fossa—is an important advantage, whereas reduced edge sharpness is disadvantageous in TSE images; both effects are more pronounced in T_2-weighted than in PD-weighted TSE images. Furthermore, the contrast of high-intensity lesions is increased in PD-weighted TSE images.

REFERENCES

1. Haase A, Frahm J, Matthaei D, Hänicke W, Merboldt KD (1986) FLASH imaging. Rapid NMR imaging using low flip angle pulses. *J Magn Reson* **67:** 258–266.
2. Oppelt A, Graumann R, Barfuß H, Fischer H, Hartl W, Schajor W (1986) FISP: eine neue Pulssequenz für die Kernspintomographie. *Electromedica* **54:** 15–18.
3. Gyngell ML (1988) The application of steady-state free precession in rapid 2DFT NMR imaging: FAST or CE-FAST sequences. *Magn Reson Imaging* **6:** 415–419.
4. Haase A (1990) Snapshot FLASH MRI. Application to T1, T2, and chemical shift imaging. *Magn Reson Med* **13:** 77–89.
5. Melki PS, Mulkern RV, Panych LP, Jolesz FA (1991) Comparing the FAISE method with conventional dual echo sequences. *J Magn Reson Imaging* **1:** 319–326.
6. Mulkern RV, Wong STS, Winalski C, Jolesz FA (1990) Contrast manipulation and artifact assessment of 2D and 3D RARE sequences. *Magn Reson Imaging* **8:** 557–566.
7. Constable RT, Anderson AW, Zhong J, Gore JC (1992) Factors influencing contrast in fast spin-echo MR-imaging. *Magn Reson Imaging* **10:** 497–511.
8. Hennig J, Nauerth A, Friedburg H (1986) RARE imaging: a fast imaging method for clinical MR. *Magn Reson Med* **3:** 823–833.
9. Hennig J, Friedburg H (1988) Clinical applications and methodological developments of the RARE technique. *Magn Reson Imaging* **6:** 391–395.
10. Mansfield P (1977) Multi-planar image formation using NMR spin echoes. *J Phys C* **10:** L55.
11. Tice HM, Jones KM, Mulkern RV, Schwartz RB, Kalina P, Ahn S, Barnes P, Jolesz F (1993) Fast spin-echo imaging of intracranial neoplasms. *J Comput Assist Tomogr* **17**(3): 425–431.
12. Ahn SS, Mantello MT, Jones KM, Mulkern RV, Melki PS, Higuchi N, Barnes PD (1992) Rapid MR imaging of the pediatric brain using the fast spin-echo technique. *AJNR* **13:** 1169–1177.
13. Jones KM, Mulkern RV, Schwartz RB, Oshio K, Barnes PD, Jolesz FA (1992) Fast spin-echo MR imaging of the brain and spine: current concepts. *Amer J Radiol* **158:** 1313–1320.
14. Jones KM, Mulkern RV, Mantello MT, Melki PS, Ahn SS, Barnes PD, Jolesz FA (1992) Brain hemorrhage: evaluation with fast spin-echo and conventional dual spin-echo images. *Radiology* **182:** 53–58.
15. Norbash AM, Glover GH, Enzman DR (1992) Intracerebral lesion contrast with spin-echo and fast spin-echo sequences. *Radiology* **185:** 661–665.
16. Bottomley PA, Foster TH, Arsinger RE, Pfeifer LM (1984) A review of normal tissue hydrogen NMR relaxation times and relaxation mechanisms from 1–100 MHz:

Dependence on tissue type, NMR frequency, temperature, species, excision, and age. *Med Phys* **11**(4): 425–448.
17. Wehrli FW, MacFall JR, Newton TH (1983) Parameters determining the appearance of NMR images. In *Advanced Imaging Techniques. Vol. II,* Newton TH and Potts DG (eds): San Anselmo: Clavadel Press.
18. Wehrli FW, Herfkens RJ, MacFall JR, Shutts D (1985) Contrast and contrast-to-noise in magnetic resonance imaging. In *An Introduction of Biomedical NMR,* Petersen SB, Muller RN, Rinck PA (eds). New York: Thieme Medical Publishers.
19. Melki PS, Mulkern RV (1992) Magnetization transfer effects in multislice RARE sequences. *Magn Reson Med* **24:** 189–195.
20. Dixon WT, Engels H, Castillo M, Sardashti M (1990) Incidential magnetization transfer contrast in standard multislice imaging. *Magn Reson Imaging* **8:** 417–422.
21. Constable RT, Gore JC (1992) The loss of small objects in variable TE imaging: implications for FSE, RARE, and EPI. *Magn Reson Med* **28:** 9–24.
22. Fellner F, Prüll C, Helmberger T, Schmitt R, Hausmann R, Obletter N, Böhm-Jurkovic H (1993) Fast spin-echo sequences with optimized proton density- and T2-contrast: A comparative study with conventional SE imaging in routine brain examinations. In *Proceedings of the Society of Magnetic Resonance in Medicine, Twelfth Annual Meeting, New York* p. 1432.
23. Fellner F, Schmitt R, Helmberger T, Prüll C, Obletter N (1993) Wertigkeit schneller Spinecho- (Turbo-Spinecho-) Sequenzen in der MR-Routinediagnostik des Zerebrums bei 1.0 Tesla. *Klinische Neuroradiologie* **3:** 111–117.